CFD and statistical analysis of flow mass ratios on temperature and pressure drops of double pipe heat exchanger

Savaş Evran[1,*,†] and Mustafa Kurt[2]

[1]*Faculty of Applied Sciences, Department of Jewelry and Jewelry Design, Marmara University, Istanbul, 348652, Turkey;* [2]*Faculty of Technology, Department of Mechanical Engineering, Marmara University, Istanbul, 34854, Turkey*

Abstract

In this numerical and statistical study, the effect of mass flow rates for shell and fluid temperature for tube on temperature and pressure drops was analyzed in double pipe heat exchanger under counterflow. Numerical calculations were performed using computational fluid dynamics (CFD) in ANSYS Fluent. Calculations were carried out according to the L8 orthogonal array with two control factors in accordance with Taguchi method. Although the different mass flow rates of the fluid passing through the shell were chosen as the first control factor, different fluid temperatures of the fluid passing through the tube were selected for the second control factor. Signal-to-noise ratio analysis was used to decide the impacts and optimum levels of the mass flow rates and fluid temperatures on temperature and pressure drop. The significance levels and contribution percentages of each variable on the temperature and pressure change occurring in the heat exchanger were calculated using analysis of variance. The accuracy of the analyses was compared numerically and statistically by comparing the obtained optimum CFD results with the estimated Taguchi results. This study can be used as a guiding research in the project and cost calculations of heat exchangers to be produced experimentally.

Keywords: Taguchi method; ANOVA; pressure; temperature; CFD; heat exchanger

*Corresponding author:
savas.evran@marmara.edu.tr Received 30 March 2023; accepted 25 May 2023

1 INTRODUCTION

Heat exchangers are tools used to transmit thermal energy, usually by using two different or the same type of fluid. Heat exchangers have been used in many sectors such as heating, ventilation and air conditioning (HVAC) systems, chemical processing plants and electricity generation plants. The basic principle of these devices is that they work by using a conductive material such as metal to transfer heat through fluid. In heat exchangers, there is a principle of operation of two fluids with different temperature values without mixing with each other. Heat transfer in heat exchangers depends on various factors such as the surface area of the exchanger, the fluid flow rate and the thermal properties of the material. There are numerous various styles of heat exchangers such as shell-and-tube heat, plate heat and spiral heat. With computational fluid dynamics (CFD) software, fluid flow and heat transfer can be accurately simulated and potential improvement areas identified. In addition, the design can be optimized to improve efficiency and performance. There are many studies evaluating heat exchangers using CFD [1–6]. In this context, many scientists have conducted studies involving heat exchangers. In a study using two different heat exchangers, pressure drop, heat transfer coefficient and fluid outlet temperature were analyzed depending on the fluid mass flow rate. ANSYS CFD software was used in the calculations. In addition, the effect of different mesh sizes on the pressure change is stated [7]. In another study, analysis of a helical coiled heat exchanger was evaluated using experimental or CFD methods under different boundary conditions, and CFD analysis was used for the accuracy of the experimental data. Water was used as fluid [8]. In another research, CFD analysis of shell-and-tube heat exchangers was carried out depending on different baffle types and the effect of mass flow rate on pressure drop was investigated. Stainless steel was used as the metal material, and four baffles were used [9]. In a study, heat transfer and fluid flow analyses of heat exchangers designed using sextant helical baffle were calculated using experimental and Contract Exchange

†, https://orcid.org/0000-0002-7512-5997
International Journal of Low-Carbon Technologies 2023, 18, 771–780

https://doi.org/10.1093/ijlct/ctad056 Advance Access publication 30 June 2023

Format (CFX) methods. In addition, the influence of mass flow rate on pressure variation was investigated [10]. Hosseini *et al.* [11] analyzed the performance of copper tubes with different surface configurations for a shell tube heat exchanger (STHE). They aimed to compare experimental data with theoretical data and suggest correlations for pressure drop and Nusselt number for the three types of tubes, as well as investigate the effect of surface configuration on heat transfer and pressure drop. Lokhande and Waghole [1] aimed to investigate the effect of varying concentrations of CuO nanoparticles in distilled water on the heat transfer characteristics of a shell-and-tube heat exchanger in counterflow configuration, and concluded that increasing the volume concentration of CuO nanoparticles results in higher overall heat transfer coefficient and rate compared with distilled water. Darbandi *et al.* [12] developed a new semi–full-scale methodology for CFD model of STHEs, which involves isolating and simulating a small block within the STHE domain for several thermal and flow situations to generate correlations that can be used to calculate the performance of the entire STHE for different conditions, thus reducing the need for full-scale simulations and facilitating the CFD simulation of large STHEs. Biçer *et al.* [13] developed a new baffle design to develop the performance of shell-and-tube heat exchangers by reducing shell-side pressure loss and improving thermal performance. You *et al.* [14] presented a numerical approach regarding the concepts of porosity and permeability to achieve the shell-side thermal hydraulic performances of an STHE with flower baffles and to demonstrate that this model is effective and economical in the thermal hydraulic design and analysis of the device. Abbasian Arani and Moradi [15] optimized the fluid flow and heat transfer of water in a segmental baffle STHE using a combined baffle and longitudinal ribbed tube configuration. They compared the found results using experimental data and numerical outcomes available in the literature to evaluate the performance of different baffle and ribbed tube configurations. In many studies [16–22], the Taguchi method has been used on heat exchangers. As can be understood from the literature review, several studies regarding different analyses of heat exchangers have been performed. However, studies dealing with the Taguchi method and CFD analysis are limited. Therefore, in this study, calculations of heat exchangers under different temperatures and mass flow rates are discussed.

2 CFD ANALYSIS

Heat exchangers generally work by transferring heat from one fluid to another to cool or heat the fluid. The efficiency of the heat transfer process that occurs is based on numerous variables such as the structure of the heat exchanger, the type of fluids and fluid velocities and temperatures. It can be used as a powerful software used in pre-production design and thermal calculations of CFD heat exchangers. CFD software plays an active role in design and cost determination on the heat exchanger. Another advantage of CFD software is that they can predict the behavior of liquids under different conditions. In addition, CFD simulations can increase efficiency and performance while reducing the time and cost required to develop new designs. The continuity, momentum, stress tensor and energy equations in ANSYS CFX are as follows, respectively [23]:

$$\frac{\partial \rho}{\partial t} + \nabla.(\rho U) = 0 \tag{1}$$

$$\frac{\partial (\rho \mathrm{U})}{\partial \mathrm{t}} + \nabla.(\rho \mathrm{UU}) = -\nabla \mathrm{p} + \nabla.\tau + S_M \tag{2}$$

$$\tau = \mu\left(\nabla \mathrm{U} + \left(\nabla \mathrm{U}^T\right) - \frac{2}{3}\delta \nabla.U\right) \tag{3}$$

$$\frac{\partial (\rho \mathrm{h})}{\partial \mathrm{t}} + \nabla.(\rho \mathrm{Uh}) = \nabla.(\mathrm{k}\nabla \mathrm{T}) + \tau : \nabla \mathrm{U} + S_E \tag{4}$$

where ρ represents density. U signifies overall velocity. ∇ denotes the nabla operator, which is used for taking spatial derivatives. p denotes static pressure. τ is the stress tensor. S_M was used as the momentum source. μ was determined to be dynamic viscosity. h, k, and S_E indicate enthalpy, thermal conductivity and energy source, respectively [24]. The temperature and pressure drop for the outer pipe (shell) is calculated with the following equations:

$$\Delta \mathrm{T}_{\mathrm{drop}} = \mathrm{T}_{\mathrm{inlet}} - \mathrm{T}_{\mathrm{outlet}} \tag{5}$$

$$\Delta \mathrm{P}_{\mathrm{drop}} = |\mathrm{P}_{\mathrm{outlet}}| - |\mathrm{P}_{\mathrm{inlet}}| \tag{6}$$

where $\Delta \mathrm{T}_{\mathrm{drop}}$ shows the temperature drop in the double pipe heat exchanger (DPHE), and it is calculated as the difference between the inlet temperature $\mathrm{T}_{\mathrm{inlet}}$ and the outlet temperature $\mathrm{T}_{\mathrm{outlet}}$. Moreover, ΔP_{drop} shows the pressure drop. In addition, $|P_{outlet}|$ and $|P_{inlet}|$ represent the absolute value of the outlet and inlet pressures. The k-epsilon realizable turbulence model was used for calculations in ANSYS Fluent. The k-ε turbulence model consists of two transport equations such as one for the turbulent kinetic energy (k) and one for the rate of dissipation in accordance with turbulent kinetic energy (ε). The equations are derived based on the Reynolds-averaged Navier–Stokes (RANS) equations and the Boussinesq hypothesis, which assumes that the Reynolds stress tensor can be modeled as a linear combination of the mean velocity gradients. The realizable k-ε model can be presented as an improved version of the standard k-ε model. This model uses a more complex equation for the length scale that is based on the flow conditions and allows for a more accurate prediction of the turbulence behavior. The transport equations for k and ε in accordance with the realizable k-ε model are [25]:

$$\frac{\partial}{\partial t}(\rho k) + \frac{\partial}{\partial x_j}\left(\rho k u_j\right) = \frac{\partial}{\partial x_j}\left[\left(\mu + \frac{\mu_t}{\sigma_k}\right)\frac{\partial k}{\partial x_j}\right] + P_k + P_b - \rho\epsilon - Y_M + S_k \tag{7}$$

$$\frac{\partial}{\partial t}(\rho \epsilon) + \frac{\partial}{\partial x_j}\left(\rho \epsilon u_j\right) = \frac{\partial}{\partial x_j}\left[\left(\mu + \frac{\mu_t}{\sigma_\epsilon}\right)\frac{\partial_\epsilon}{\partial x_j}\right] + \rho C_1 S_\epsilon - \rho C_2 \frac{\epsilon^2}{k + \sqrt{\nu\epsilon}} + C_{1\epsilon}\frac{\epsilon}{k}C_{3\epsilon}P_b + S_\epsilon \tag{8}$$

$$c_1 = \max\left[0.43, \frac{\eta}{\eta+5}\right], \eta = S\frac{k}{\epsilon}, S = \sqrt{2S_{ij}}S_{ij} \quad (9)$$

$$\mu_t = \rho C_\mu \frac{k^2}{\epsilon} \quad (10)$$

where ρ, t, x, u, μ and μ_t define the density of the fluid, time, the spatial coordinate, the velocity vector, the molecular viscosity and the turbulent viscosity, respectively. The terms P_k and ε represent the production and dissipation of k and ε, respectively. The constants σ_k and σ_ϵ are model constants that determine the behavior of the model near walls and in the free stream. The constants $C_{1\epsilon}$ and $C_{3\epsilon}$ are also model constants that control the behavior of the model in regions of high turbulence intensity.

$$C_\mu = \frac{1}{A_0 + A_s\frac{kU^*}{\epsilon}} \quad (11)$$

$$U^* \equiv \sqrt{S_{ij}S_{ij} + \tilde{\Omega}_{ij}\tilde{\Omega}_{ij}} \quad (12)$$

$$\tilde{\Omega}_{\iota j} = \Omega_{ij} - 2_{\epsilon_{ijk}}\omega_k \quad (13)$$

$$\Omega_{ij} = \bar{\Omega}_{ij} - \epsilon_{ijk}\omega_k \quad (14)$$

where, $\tilde{\Omega}_{\iota j}$ represents the tilde notation for the overall rotation speed tensor detected around a rotating reference frame with the angular speed represented by the ω_k value.

$$A_0 = 4.04, A_s = \mathrm{A_S} = \sqrt{6}\cos\phi \quad (15)$$

$$\varnothing = \frac{1}{3}\cos^{-1}\left(\sqrt{6W}\right), W = \frac{S_{ij}S_{jk}S_{ki}}{\tilde{S}^3}, \tilde{S} = \sqrt{S_{ij}S_{ij}}, S_{ij} = \frac{1}{2}\left(\frac{\partial u_j}{\partial x_i} + \frac{\partial u_i}{\partial x_i}\right) \quad (16)$$

$$C1_\epsilon = 1.44, C_2 = 1.9, \sigma_k = 1.0, \sigma_e = 1.2 \quad (17)$$

where C_μ represents a function that relates to the angular speed of turning for the system and the turbulence fields, namely k and ε. It takes into account the overall tension and rotational speeds. A_0 and A_s are used as model constants.

2.1 Modeling of heat exchanger

DPHE was examined under counterflow. Mass flow rates were chosen for the shell and tube as variable parameters. The length, tube diameter and shell diameter of the heat exchanger were determined as 2000, 500 and 100 mm, respectively. The thickness for the shell and tube is 1 mm. In CFD analysis, frictions and gravity in the heat exchanger are neglected. Convection approach was applied for the tube. The realizable k-ε model was used as viscous model. In addition, enhanced wall treatment was used as near-wall treatment. Water-liquid was considered as fluid and properties such as density, specific heat, thermal conductivity and viscosity were determined as 998.2 kg/m^3, 4182 j/kg-K, 0.6 W/m-K and 0.001003 kg/m-s, respectively [26]. In addition, hot and cold outlets were selected as outflows. Absolute criteria of residuals such as continuity, x-velocity, y-velocity, z-velocity, energy, k, and epsilon were taken as 10^{-6}. Each analysis was completed in 2000 iterations. In mesh operations, growth rate was selected as 1.2, and defeature size was determined as default. Smooth transition in inflation option was chosen. Target skewness was used as 0.9, and smoothing was assumed as high.

2.2 Statistical approach

The Taguchi method is often used in the manufacturing industry as a powerful statistical approach to improve quality and reduce costs. Identifying and controlling the factors that have the greatest impact on the final results can allow designing parameters that are less sensitive to variation. In this study, determination of optimum mass flow rates was investigated. The Taguchi method signal-to-noise (S/N) ratio analysis involves designing experiments to test the effects of different controllable factors on the S/N ratio and using statistical methods such as analysis of variance (ANOVA) and regression analysis to identify the most significant factors and their optimal levels. In this context, whereas the inlet fluid temperatures for tube are 343 and 363 K for tube, mass flow rates are determined as 1, 1.3, 1.6 and 1.9 kg/s for the shell. Mass flow rate is taken as 8 kg/s for the shell. The variables used according to the Taguchi L8 orthogonal array and the levels of these variables are given in Table 1.

In Taguchi S/N ratio analysis, the aim is to minimize the impacts of noise factors on the items or process while maximizing the impacts of the signal parameter. The signal parameters are the controllable design or process variables that have a direct effect on the quality of the items or process, whereas the noise factors are the uncontrollable variables that affect the quality of the product or process but are difficult or impossible to control. CFD analyses were performed according to the L8 orthogonal array. This array consists of two different parameters. The first variable parameter consists of two levels, whereas the second variable consists of four levels. To compute the maximum temperature and pressure change in the heat exchanger, the 'bigger is better' approach in the Taguchi method was used. This type of S/N ratio is used when the objective is to maximize the output variable such as yield, strength or throughput. In this case, the S/N ratio is calculated as the negative logarithm of the squared deviation of the output from the nominal value. Considering this approach, the equation is as follows [27]:

$$(\mathrm{S/N})_{\mathrm{LB}} = -10.\log\left(\mathrm{n}^{-1}\sum_{\mathrm{i}=1}^{\mathrm{n}}\left(\mathrm{y_i^2}\right)^{-1}\right) \quad (21)$$

where n describes the number of CFD calculations of temperature and pressure drops for a trial and $\mathrm{y_i}$ states $\mathrm{i^{th}}$ value calculated. In addition, the usability of each control factor for the Taguchi estimated outcome was determined using ANOVA. In the Taguchi

Table 1. *Variable parameters for different levels.*

Variable Parameters	Symbols	Units	Level 1	Level 2	Level 3	Level 4
Mass flow rate for shell	A	kg/s	1.0	1.3	1.6	1.9
Fluid temperature for tube	B	K	343	363	—	—

Table 2. *Results for CFD and S/N ratios.*

Runs	Variable Factors		Results			
	Mass Flow Rate for Tube	Fluid Temperature for Tube	Temperature Drop for Shell ΔT_{drop} (K)	S/N ratio η (dB)	Pressure Drop for Shell ΔP_{drop} (Pa)	S/N ratio η (dB)
1	1.0 kg/s	343 K	21.47882	26.6402	283.1175	49.0393
2	1.0 kg/s	363 K	31.46695	29.9571	282.9934	49.0355
3	1.3 kg/s	343 K	20.79067	26.3574	305.9572	49.7132
4	1.3 kg/s	363 K	30.46075	29.6748	305.9572	49.7132
5	1.6 kg/s	343 K	19.47379	25.7890	324.2959	50.2188
6	1.6 kg/s	363 K	28.53137	29.1065	324.2959	50.2188
7	1.9 kg/s	343 K	18.87750	25.5189	345.4196	50.7669
8	1.9 kg/s	363 K	27.65773	28.8363	345.4196	50.7669
Overall mean ($\overline{T_i}$)			24.84220	—	314.68205	—

method, ANOVA is used to determine the results of a series of calculations that are carried out to select the optimal settings for the different variables. ANOVA defines the extent to which each variable affects the quality of the product or process, as well as any interactions between the factors.

3 RESULTS AND DISCUSSIONS

In the CFD analysis, the simulation is run with various input parameters to analyze the impact of these variables on the temperature and pressure drops of the fluid flow system. The Taguchi technique was used to conclude the optimal combination of input parameters or design variables that will result in the best performance of the fluid flow system. The Taguchi method was used to reduce the number of simulations required by selecting a small number of parameter combinations to simulate. The CFD results obtained according to the L8 orthogonal array and the corresponding S/N ratios are presented in Table 2.

According to Table 2, the mean values for the temperature drop and the pressure drop for the shell are calculated as $\overline{T_{\Delta T_S}}$ = 24.8422 K and $\overline{T_{\Delta P_S}}$ = 314.68205 Pa, respectively. The CFD results calculated according to the L8 orthogonal array due to the temperature and pressure drops occurring in DPHE are given in Figures 1–8 and Figures 9–16, respectively.

Figures 1–18 show that the lowest temperature value of the fluid in the shell is detected in the fluid inlet region, whereas the highest temperature value is observed in the shell exit region. The fluid temperature change takes place with an inhomogeneous change from the inlet region to the outlet region.

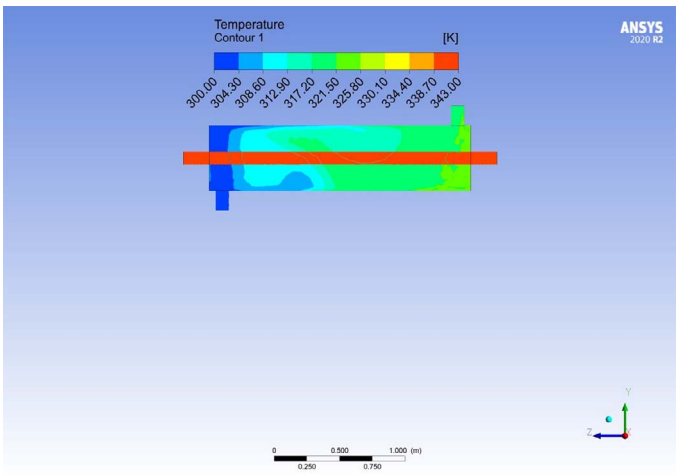

Fig. 1. *First CFD result for temperature.*

Figures 9–16 show that the pressure variation of the fluid in the shell does not create a homogeneous distribution. Depending on the absolute value, the maximum static pressure occurs in the shell exit region of the fluid.

3.1 Determination of optimal levels of variables

The Taguchi method and ANOVA are two statistical techniques used in engineering and manufacturing to improve product quality and reduce variability. ANOVA, on the other hand, is a statistical technique used to analyze the variation in a response variable due to various parameters or sources of variation. It involves partitioning the total variation for the response variable into

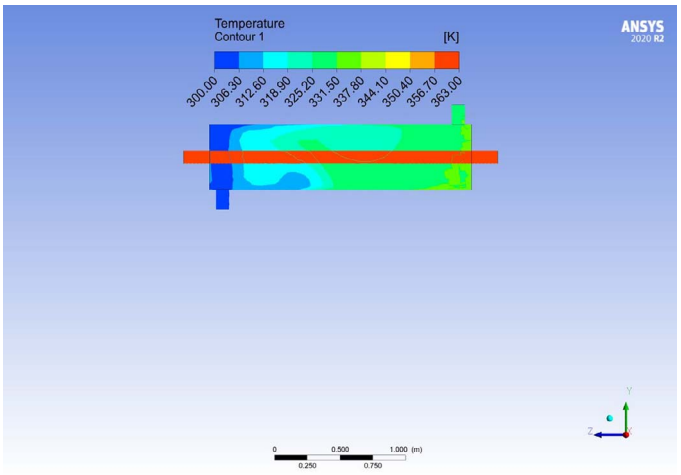

Fig. 2. *Second CFD result for temperature.*

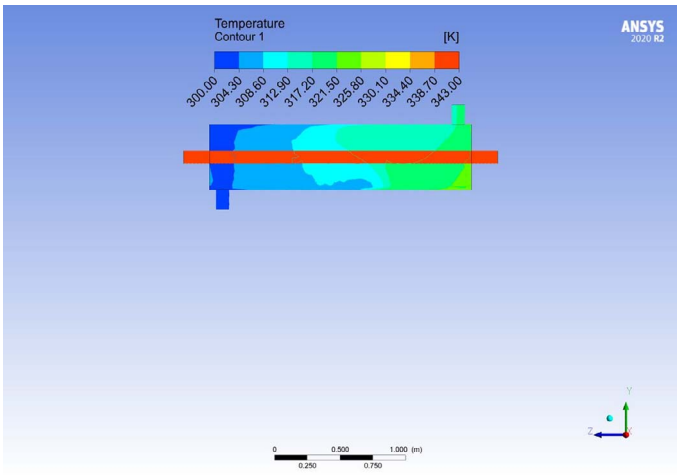

Fig. 5. *Fifth CFD result for temperature.*

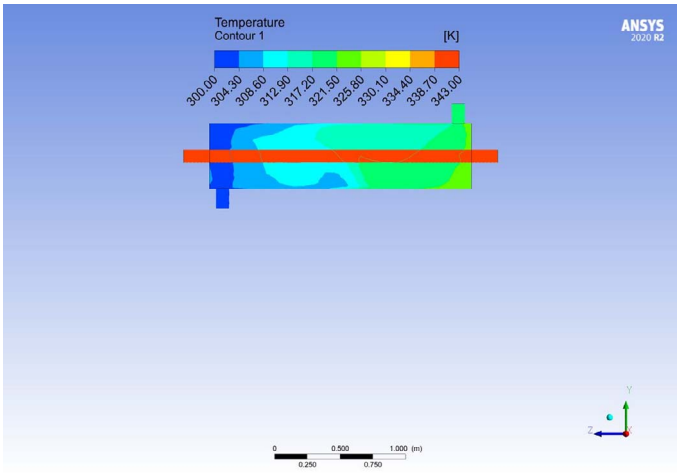

Fig. 3. *Third CFD result for temperature.*

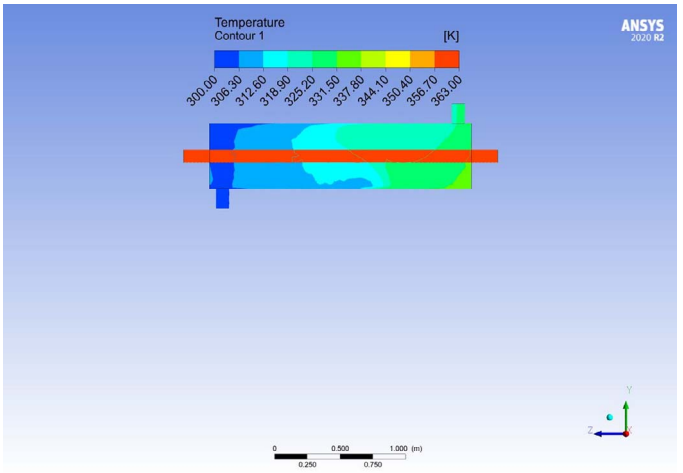

Fig. 6. *Sixth CFD result for temperature.*

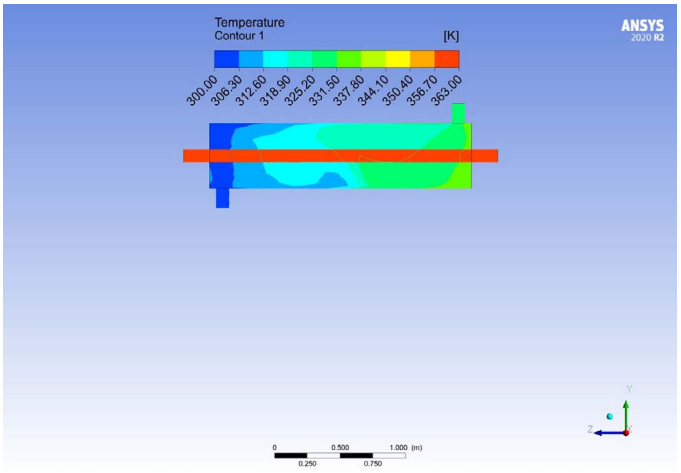

Fig. 4. *Fourth CFD result for temperature.*

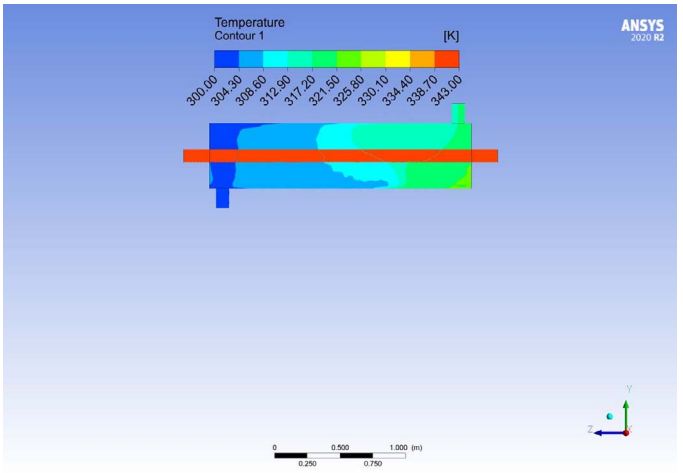

Fig. 7. *Seventh CFD result for temperature.*

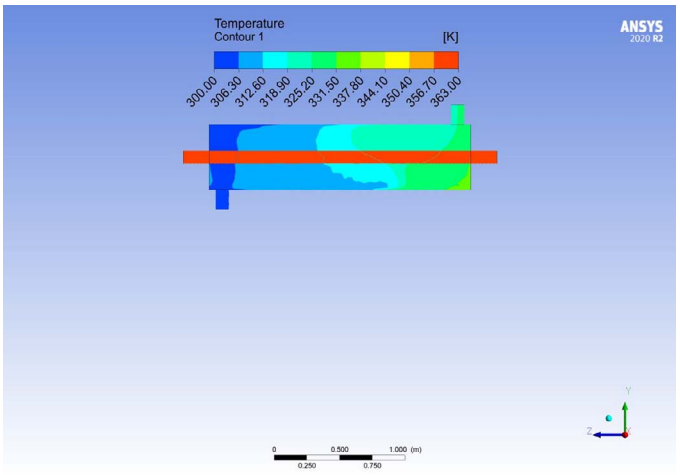

Fig. 8. *Eighth CFD result for temperature.*

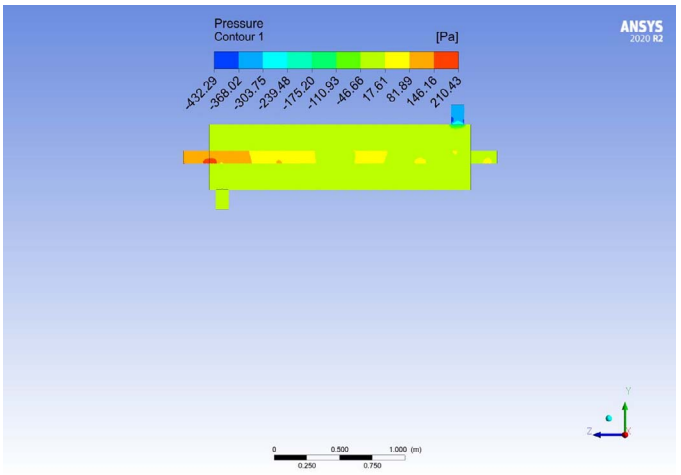

Fig. 11. *Third CFD result for pressure.*

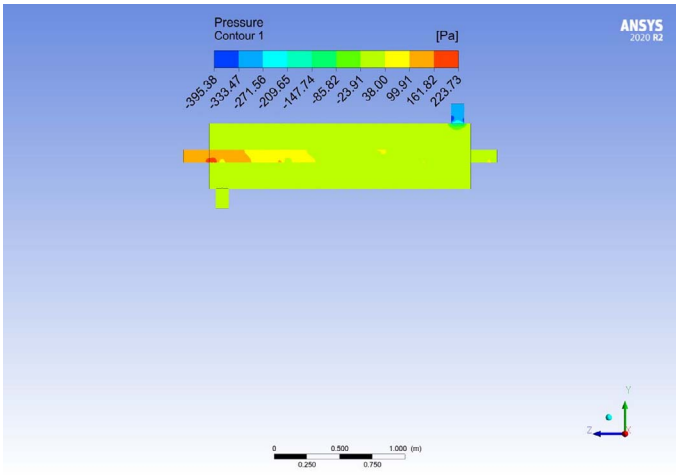

Fig. 9. *First CFD result for pressure.*

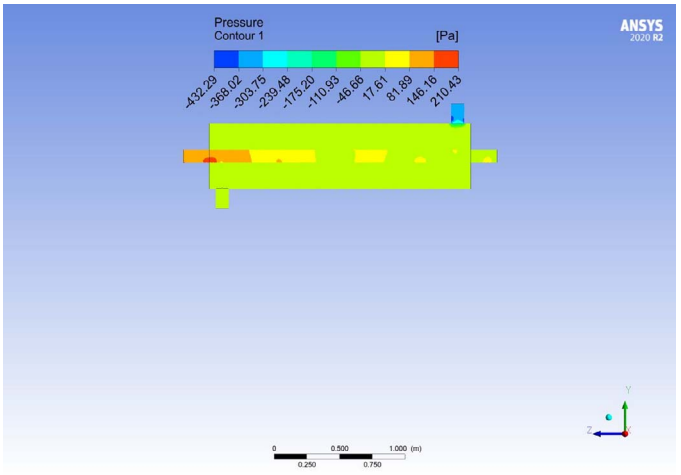

Fig. 12. *Fourth CFD result for pressure.*

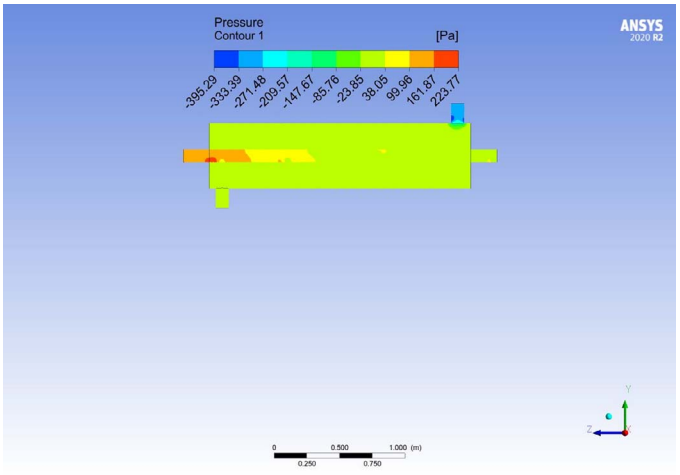

Fig. 10. *Second CFD result for pressure.*

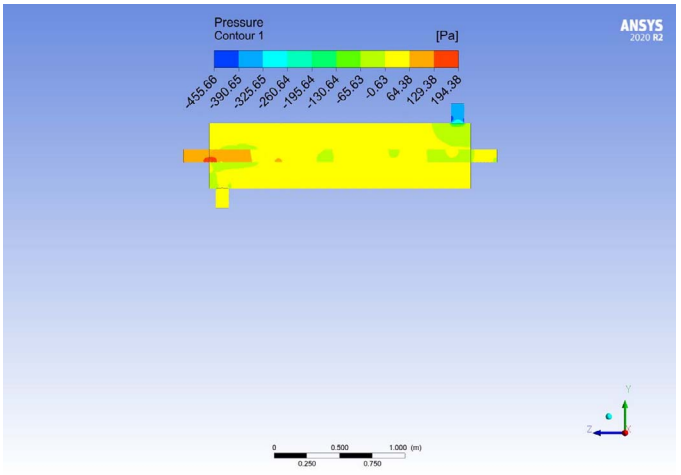

Fig. 13. *Fifth CFD result for pressure.*

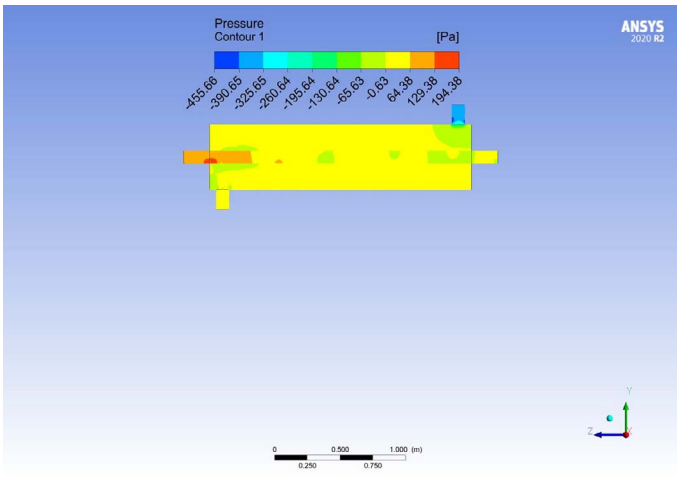

Fig. 14. *Sixth CFD result for pressure.*

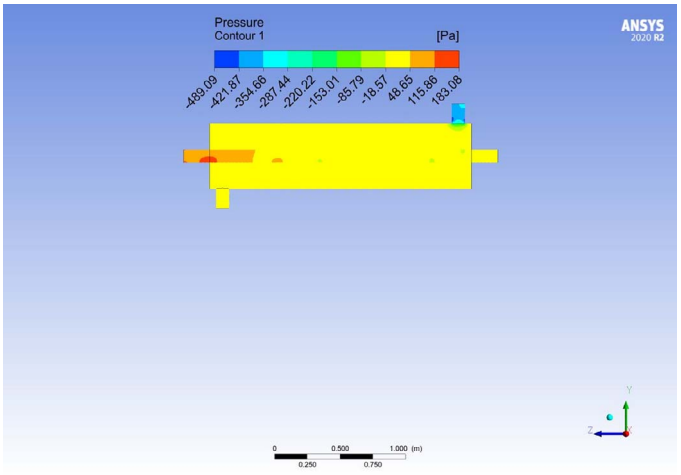

Fig. 15. *Seventh CFD result for pressure.*

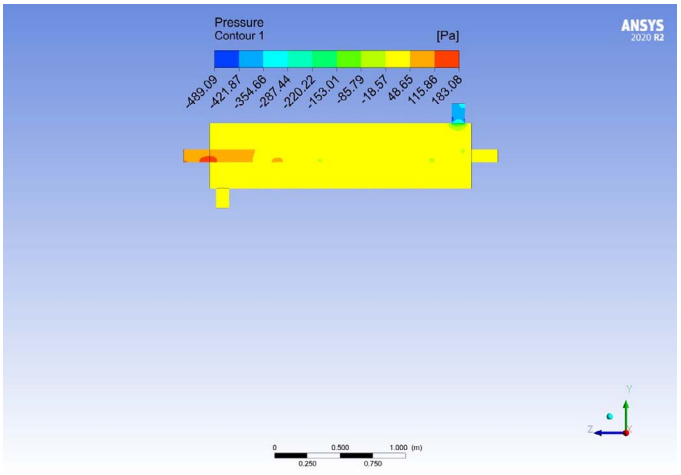

Fig. 16. *Eighth CFD result for pressure.*

different components that can be attributed to different factors or sources. ANOVA can be used to test the significance of the effects of different factors and to identify which factors have the greatest impact on the response. ANOVA was used to determine the contribution rates and importance levels of mass flow rate and fluid temperature to the shell-and-tube heat exchanger efficiency. ANOVA results performed at 95% confidence level are given in Table 3.

It can be seen from Table 3 that the most effective variables on the temperature drop in the shell are fluid temperature with 92.93 effect and mass flow rate with 6.83 effect, respectively. In addition, it is understood from the P value (< 0.05) that both variables are important variables. For the pressure drop in the shell, the mass flow rate was determined as the important variable, whereas the fluid temperature was determined as the insignificant variable. Therefore, it has been calculated that the mass flow rate has 100% effect on the pressure drop. In addition, because the P value is less than 0.05, it was used as an effective variable in determining the optimum levels. The Taguchi method S/N ratio analysis is a statistical approach used to calculate and optimize the performance of a response by analyzing the relationship between the controllable factors and the variability or noise in the output. The numerical data obtained from the CFD analysis results were converted into S/N ratio values. Thus, the results of the mean numerical and statistical temperature and pressure drop for each level of each variable were calculated. The results achieved are listed in Table 4.

Table 4 shows that the optimum levels on temperature drop are the first level of mass flow rate and the second level of fluid temperature. For the pressure drop, the optimum levels are the fourth level of the mass flow rate. However, because there is no contribution from the fluid temperature, there is no optimum level.

3.2 Impact on temperature and pressure drops

To realize the effects of each variable on temperature and pressure drop due to different levels, CFD calculations were carried out according to the Taguchi L8 orthogonal array. For each level, the mean CDF results corresponding to the variables and the corresponding S/N ratio values were calculated. These values are presented in Table 4. The graph based on the average S/N ratio data in accordance with temperature and pressure drop for shell is drawn in Figure 17 and 18, respectively.

Figure 17 shows that an increase in mass flow rate for the fluid in the shell is observed as a decrease in temperature. This finding can be explained by the fact that the increase in the mass flow rate of the fluid is due to the fact that the fluid, which continues to circulate in the shell, cannot reach the sufficient temperature. This is because the increase in fluid mass flow rate is inversely proportional to the increase in fluid temperature. However, an increase in fluid temperature from 343 to 363 K causes an increase in temperature drop. This finding may be described by the fact that the temperature increase is directly proportional to the temperature change. In Figure 18, it has been determined that an

Table 3. *ANOVA result for temperature and pressure drops.*

Source	DF	Temperature Drop in Shell					Pressure Drop in Shell				
		Seq SS	Adj MS	F	*P*	% Effect	Seq SS	Adj MS	F	*P*	% Effect
A	3	12.915	4.305	28.15	0.011	6.83	4227.2	1409.1	731817.2	0	100
B	1	175.744	175.744	1149.27	0	92.93	0	0	1	0.391	0
Error	3	0.459	0.153			0.24	0	0			0
Total	7	189.117				100	4227.2				100
R-Sq = 99.76% and R-Sq(adj) = 99.43%							R-Sq = 100% and R-Sq(adj) = 100%				

Table 4. *Average response for each levels of each variable parameter.*

Level	Temperature Drop for Shell				Pressure Drop for Shell			
	S/N ratios in dB		Mean in K		S/N ratios in dB		Mean in Pa	
	A	B	A	B	A	B	A	B
1	28.3	26.08	26.47	20.16	49.04	49.93	283.10	314.70
2	28.02	29.39	25.63	29.53	49.71	49.93	306.00	314.70
3	27.45		24.00		50.22		324.30	
4	27.18		23.27		50.77		345.40	
Delta	1.12	3.32	3.21	9.37	1.73	0	62.40	0
Rank	2	1	2	1	1	2	1	2

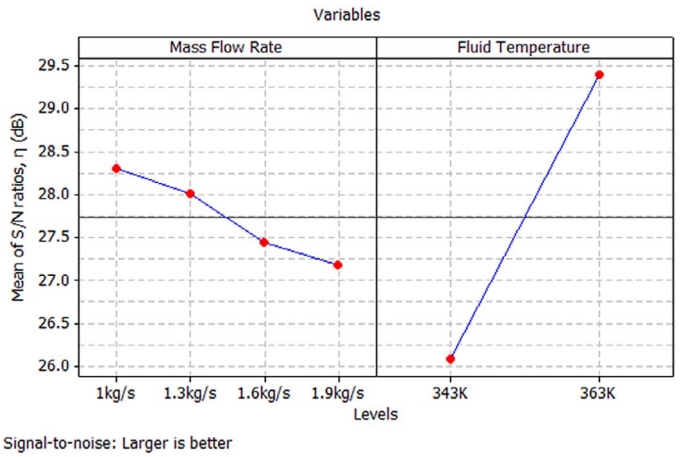

Fig. 17. *Effect of variables at different levels for temperature drop.*

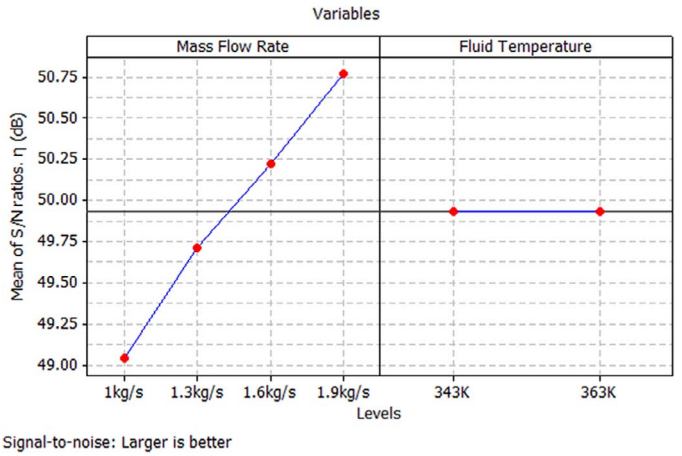

Fig. 18. *Effect of variables at different levels for pressure drop.*

increase in the mass flow rate from 1 to 1.9 kg/s for the fluid in the shell causes an increase in the pressure drop. The reason for this situation is that the increase in the mass flow rate of the fluid creates pressure in the shell fluid outlet region. However, the increase in fluid temperature from 343 to 363 K did not cause any change on the pressure drop. In other words, the change in fluid temperature inside the acceptance has no effect on the pressure drop.

3.3 Estimation of temperature and pressure drops

To predict the optimal values of temperature and pressure drops for shell, the optimal levels of significant variables such as mass flow rate and fluid temperature were used. The significance levels of the variables were determined according to ANOVA, which was realized at the 95% confidence level. Using the optimum levels of each important variable, the estimated temperature and pressure drops can be calculated as follows [27]:

$$\mu_k = \overline{A_j} + \overline{B_j} - \overline{T_a} \tag{3}$$

where $\overline{T_a}$ denotes the average means for temperature and pressure drops in accordance with L8 orthogonal array in the Taguchi method. $\overline{T_a}$ data for temperature and pressure drops were calculated as $\overline{T_{\Delta T_S}}$ = 24.8422 K and $\overline{T_{\Delta P_S}}$ = 314.682 Pa, respectively. For temperature drop, $\overline{A_1}$ = 26.47 and $\overline{B_2}$ = 29.53 show the average CFD data at the first level of the first variable, which is the mass flow rate, and the second level of second variable, which is the fluid

Table 5. *Comparison of optimal estimation and CFD results.*

Responses	Combination	Predicted Result	CFD Result	± Residual	% Different
Temperature drop	A_1B_2	31.1578 K	31.4669 K	03091	0.98%
Pressure drop	A_4B_{1or2}	345.0179 Pa	345.4196 Pa	0.4017	0.11%

temperature, respectively. For pressure drop, $\overline{A_4}$ = 345.40 indicate the average CFD data at the fourth level of the first variable, which is the mass flow rate. $\overline{B_{1or2}}$ = 314.70 is calculated. Substituting CFD data calculated of various terms in Equation 3, $\mu_{\Delta T_S}$ and $\mu_{\Delta P_S}$ are calculated as 3.7720 and 834.6536, respectively. Taguchi estimation and CFD results based on optimum levels are given in Table 5.

As seen in Table 5, the optimum results of estimation and CFD calculations for temperature are calculated as 31.1578 and 31.4669 K, respectively. In addition, the optimum results of the estimation and CFD analyses on the pressure drop were calculated as 345. 0179 and 345.4196 Pa, respectively. The percentage differences obtained for temperature and pressure drop were calculated as 0.98 and 0.11%, respectively. Obtaining a very low difference between both results shows that the numerical results are consistent and significant with the statistical results.

4 CONCLUSIONS

In this study, the effects of different mass flow rate of the fluid passing through the shell and different temperatures of the fluid passing through the tube of DPHE on the temperature and pressure drop of the fluid passing through the shell were investigated using CFD and Taguchi methods. The flow in the heat exchanger is considered as crossflow. CFD calculations were performed using ANSYS software. Analyses were carried out according to the Taguchi L8 orthogonal array. The mass flow rates of the fluid passing through the shell were considered as 1, 1.3, 1.6 and 1.9 kg/s, respectively, and were chosen as the levels of the first variable. The temperature of the fluid passing through the tube was assigned as 343 and 363 K, respectively, and the levels of the second variable were determined. S/N ratio analysis was used to evaluate the effects of different levels of each variable on temperature and pressure drop. The significance levels of the variables were determined using ANOVA. According to this CFD and statistical study, the increase in the mass flow rate of the fluid passing through the shell increases the pressure drop while decreasing the temperature drop. The increase in the temperature of the fluid passing through the tube from 343 to 363 K increases the temperature drop of the fluid passing through the shell, but does not have any effect on the pressure drop. According to S/N ratio analysis, the optimum levels for maximum temperature and pressure drops are obtained using the first level and the fourth level of the mass flow rate, respectively. It is obtained using the second level of fluid temperature passing through the tube. ANOVA results showed that although the mass flow rate was determined as a significant variable on temperature and pressure drops, the fluid temperature in the tube was determined as a significant variable on the temperature drop but insignificant on the pressure drop. The percentage differences determined for temperature and pressure drop were found to be 0.98 and 0.11%, respectively.

REFERENCES

[1] Lokhande AA, Waghole DR. CFD investigation on heat transfer enhancement in shell and tube heat exchanger using copper oxide nano liquid. *Materials Today: Proceedings* 2022;**64**:499–505.

[2] Somasekhar K, Malleswara Rao KND, Sankararao V *et al.* A CFD investigation of heat transfer enhancement of shell and tube heat exchanger using Al2o3-water nanofluid. *Materials Today: Proceedings* 2018;**5**:1057–62.

[3] Ozden E, Tari I. Shell side CFD analysis of a small shell-and-tube heat exchanger. *Energy Convers Manag* 2010;**51**:1004–14.

[4] Bahiraei M, Naseri M, Monavari A. A CFD study on thermohydraulic characteristics of a nanofluid in a shell-and-tube heat exchanger fitted with new unilateral ladder type helical baffles. *International Communications in Heat and Mass Transfer* 2021;**124**:1–17.

[5] Cruz PAD, Yamat E-JE, Nuqui JPE, Soriano AN. Computational fluid dynamics (CFD) analysis of the heat transfer and fluid flow of copper (II) oxide-water nanofluid in a shell and tube heat exchanger. *Digital Chemical Engineering* 2022;**3**:1–14.

[6] Yang D, Khan TS, Al-Hajri E *et al.* Geometric optimization of shell and tube heat exchanger with interstitial twisted tapes outside the tubes applying CFD techniques. *Appl Therm Eng* 2019;**152**:559–72.

[7] İnan AT, Köten H, Kartal MA. CFD analysis and comparison of conventional type and perforated plate type shell tube heat exchangers. *International Journal of Low-Carbon Technologies* 2022;**17**:1280–91.

[8] Jayakumar JS, Mahajani SM, Mandal JC *et al.* Experimental and CFD estimation of heat transfer in helically coiled heat exchangers. *Chem Eng Res Des* 2008;**86**:221–32.

[9] Bichkar P, Dandgaval O, Dalvi P *et al.* Study of shell and tube heat exchanger with the effect of types of baffles. *Procedia Manufacturing* 2018;**20**:195–200.

[10] Cao X, Du T, Liu Z *et al.* Experimental and numerical investigation on heat transfer and fluid flow performance of sextant helical baffle heat exchangers. *Int J Heat Mass Transf* 2019;**142**:1–13.

[11] Hosseini R, Hosseini-Ghaffar A, Soltani M. Experimental determination of shell side heat transfer coefficient and pressure drop for an oil cooler shell-and-tube heat exchanger with three different tube bundles. *Appl Therm Eng* 2007;**27**:1001–8.

[12] Darbandi M, Abdollahpour M-S, Hasanpour-Matkolaei M. A new developed semi-full-scale approach to facilitate the CFD simulation of shell and tube heat exchangers. *Chem Eng Sci* 2021;**245**:1–11.

[13] Biçer N, Engin T, Yaşar H *et al.* Design optimization of a shell-and-tube heat exchanger with novel three-zonal baffle by using CFD and Taguchi method. *Int J Therm Sci* 2020;**155**:1–11.

[14] You Y, Fan A, Huang S, Liu W. Numerical modeling and experimental validation of heat transfer and flow resistance on the shell side of a shell-and-tube heat exchanger with flower baffles. *Int J Heat Mass Transf* 2012;**55**:7561–9.

[15] Abbasian, Arani AA, Moradi R. Shell and tube heat exchanger optimization using new baffle and tube configuration. *Appl Therm Eng* 2019;**157**:1–11.
[16] Tang L-H, Tan S-C, Gao P-Z, Zeng M. Parameters optimization of fin-and-tube heat exchanger with a novel vortex generator fin by Taguchi method. *Heat Transfer Engineering* 2016;**37**:369–81.
[17] Zeng M, Tang LH, Lin M, Wang QW. Optimization of heat exchangers with vortex-generator fin by Taguchi method. *Appl Therm Eng* 2010;**30**:1775–83.
[18] Du T, Du W, Che K, Cheng L. Parametric optimization of overlapped helical baffled heat exchangers by Taguchi method. *Appl Therm Eng* 2015;**85**:334–9.
[19] Majid Etghani M, Amir Hosseini Baboli S. Numerical investigation and optimization of heat transfer and exergy loss in shell and helical tube heat exchanger. *Appl Therm Eng* 2017;**121**:294–301.
[20] Wang H, Liu Y-w, Yang P *et al.* Parametric study and optimization of H-type finned tube heat exchangers using Taguchi method. *Appl Therm Eng* 2016;**103**:128–38.
[21] Jamshidi N, Farhadi M, Ganji DD, Sedighi K. Experimental analysis of heat transfer enhancement in shell and helical tube heat exchangers. *Appl Therm Eng* 2013;**51**:644–52.
[22] Chamoli S, Yu P, Kumar A. Multi-response optimization of geometric and flow parameters in a heat exchanger tube with perforated disk inserts by Taguchi grey relational analysis. *Appl Therm Eng* 2016;**103**:1339–50.
[23] ANSYS. Ansys CFX-Solver Theory Guide, Release 14.0. 2011.
[24] Garud KS, Seo J-H, Cho C-P, Lee M-Y. Artificial neural network and adaptive neuro-fuzzy Interface system modelling to predict thermal performances of thermoelectric generator for waste heat recovery. *Symmetry* 2020;**12**:1–30.
[25] ANSYS. Ansys Fluent User's Guide. Inc, Canonsburd, PA 2015.
[26] ANSYS. *Fluent Software Material Database*. Canonsburg, PA: ANSYS Inc., 2021.
[27] Ross PJ. *Taguchi Techniques for Quality Engineering* 2nd edn. New York, USA: McGraw-Hill International Editions, 1996.